[CANCER RESEARCH 48, 676–681, February 1, 1988]

In Vivo ^{31}P Nuclear Magnetic Resonance Spectroscopy of Subcutaneous 9L Gliosarcoma: Effects of Tumor Growth and Treatment with 1,3-Bis(2-chloroethyl)-1-nitrosourea on Tumor Bioenergetics and Histology[1]

R. Grant Steen, Rafael J. Tamargo, Kathy A. McGovern, S. Sunder Rajan, Henry Brem, Janna P. Wehrle, and Jerry D. Glickson[2]

Departments of Radiology [R. G. S., K. A. M., S. S. R., J. P. W., J. D. G.], Neurological Surgery [R. J. T., H. B.], Oncology [H. B.], and Biological Chemistry [J. D. G.], The Johns Hopkins University School of Medicine, Baltimore, Maryland 21205

ABSTRACT

***In vivo* ^{31}P nuclear magnetic resonance spectroscopy was used to examine the bioenergetics of the rat 9L gliosarcoma during untreated growth and in response to chemotherapy with 1,3-bis(2-chloroethyl)-1-nitrosourea. Tumor growth was associated with a decline in the phosphocreatine and nucleoside triphosphate resonances, consistent with an increase in tumor hypoxia during untreated growth. Following chemotherapy with 1,3-bis(2-chloroethyl)-1-nitrosourea (10 mg/kg), tumor levels of phosphocreatine and nucleoside triphosphate rebounded while the level of inorganic phosphate in the tumor declined. Histological comparison of treated and untreated tumor sections 4 days posttreatment showed that the treated tumor had a lower proportion of necrotic cells, a higher proportion of viable cells, and a 5-fold higher level of interstitial space than the control tumor.**

INTRODUCTION

Nuclear magnetic resonance spectroscopy provides a noninvasive method for monitoring tumor bioenergetics and response to therapy (1–5). Phosphorylated compounds free in solution at concentrations of 1 mM or greater can potentially be detected *in vivo* using ^{31}P NMR[3] spectroscopy (6). Critical bioenergetic metabolites such as NTP (ATP, UTP, and similar compounds), PCr, and P_i are thus easily observed *in vivo*, and a variety of phosphomonoester and phosphodiester compounds have also been detected (7, 8).

^{31}P NMR spectroscopy has been used to monitor tumor growth and response to therapy in several experimental tumor lines (1, 3, 9). Most tumors become less metabolically active with increasing size (1–3, 10). Tumor response to various types of chemotherapy and X-irradiation therapy often involves a reversal of the changes seen during untreated tumor progression; the treated tumor appears more highly energized than untreated control tumors. This metabolic reenergization has been observed by NMR in the mammary 16/C adenocarcinoma treated with Adriamycin or X-irradiation (2) and in the RIF-1 fibrosarcoma treated with cyclophosphamide (3, 11). However, to our knowledge, no attempt has yet been made to correlate observed spectral changes with histological analysis of tumor tissues.

Here we report the results of *in vivo* NMR studies of the well-characterized rat 9L gliosarcoma and its response to chemotherapy. Spectra derived from the treated tumors clearly showed a relative increase in levels of high energy phosphates when compared to untreated controls. Spectral changes observed during untreated tumor growth and changes in the tumor following treatment were quantified. Hypotheses to explain these changes were tested by quantitative histological analysis of treated and control tumors. Histological analyses suggest that the spectral changes observed in treated tumors are a consequence of a decrease in the proportion of necrotic cells and an increase in the proportion of viable cells and interstitial space.

MATERIALS AND METHODS

Tumor Implantation. For the establishment of s.c. 9L tumors, 10-day-old Fischer 344 rats were inoculated in the right flank with 10^6 cultured 9L cells in 0.2 ml of growth medium. Young rats were used for these experiments because of size limitations imposed by the diameter of the magnet bore.

Chemotherapy. BCNU was provided by the Drug Synthesis and Chemistry Branch of the Division of Cancer Treatment (National Cancer Institute). Twelve days after tumor implantation, rats were treated with BCNU (10 mg/kg) in 4% ethanol-saline injected i.p. Control rats were sham-treated with equal volumes of the carrier solution. NMR spectra were obtained from each rat at 1 and 4 days posttreatment.

Measurement of Tumor Volume. Tumor volume was estimated by measuring tumor dimensions along the long axis of the tumor and across the tumor at the widest point. Tumor volume was calculated by the equation (12, 13):

$$\text{Volume} = 0.5\ (\text{length} \times \text{width}^2)$$

***In Vivo* NMR Spectroscopy of s.c. Tumors.** NMR spectra were taken using a Bruker AM 360 multinuclear spectrometer (8.5 T/8.9-cm bore) equipped with an Aspect 3000 computer. Home-built probes with a solenoidal radiofrequency coil (14), doubly tuned to proton and phosphorus (15), were used.

Rats were anesthetized by i.p. injection of a ketamine/xylazine cocktail (ketamine HCl, 50 mg/kg; xylazine, 5 mg/kg; in 14% ethanol and normal saline). Tumor spectra were obtained by placing a three-turn solenoidal radiofrequency coil around the tumor while the body of the anesthetized animal was isolated from the receiver coil by a Faraday shield (1). All spectra were acquired at 145.8 MHz using a 60-degree pulse (7 μs) and a 3-s recycle time. All spectra were collected according to the same spectroscopic parameters. No corrections were made for saturation effects. Acquisitions of 1K points over a sweep width of 12 KHz yielded spectra with a signal:noise ratio for α-NTP of greater than 20 within 10 min. Spectra were analyzed by integrating resonance areas with a Lorentzian line-fitting program (GLINFIT; Bruker Instruments, Inc.). To compare spectra, ratios of peak areas of interest were calculated. Comparisons between treated and untreated tumor spectra were made by *t* test analysis of mean peak area ratios.

Received 8/10/87; revised 10/26/87; accepted 10/30/87.

The costs of publication of this article were defrayed in part by the payment of page charges. This article must therefore be hereby marked *advertisement* in accordance with 18 U.S.C. Section 1734 solely to indicate this fact.

[1] Supported in part by USPHS Grants CA 39958 and CA 44703 from The NIH (to J. D. G.), NIH Grant NS 01508-01 and Grant IN-11W from the American Cancer Society (to H. B.), NRSA Traineeship CA 09199 from the NIH (to R. G. S.), and by the Association for Brain Tumor Research (to R. J. T.).

[2] To whom requests for reprints should be addressed.

[3] The abbreviations used are: NMR, nuclear magnetic resonance; PCr, phosphocreatine; BCNU, 1,3-bis(2-chloroethyl)-1-nitrosourea; PME, phosphomonoester; PEt, phosphorylethanolamine; PCh, phosphorylcholine; i.t., intratumoral; P_i, inorganic phosphate.

Histology. Four days following chemotherapy, treated and untreated 9L tumors were fixed in 10% phosphate-buffered formalin within 1 min of animal sacrifice. Fixed tumors were embedded in paraffin, and sections taken from the widest point of each tumor were stained with hematoxylin-eosin.

The percentage of cystic area per tumor was quantified by tracing slide mount sections onto acetate film. The film overlying macroscopically solid tumor and cystic tumor regions was then cut out and weighed. Four replicate tracings were made per cross-section.

Treated and control slide mounts were examined and scored for tumor cell morphology using a Nikon binocular compound microscope. Noncystic regions of all specimens were examined at × 400 and scored for number of vascular elements per microscopic field, number of cells per field, and average vessel lumen diameter (measured by ocular micrometer). These measurements permitted calculation of vessel cross-sectional area per field and number of tumor cells per unit vessel cross-sectional area.

To quantify tumor micromorphology in noncystic tumor regions, randomly chosen points on the microscopic field were scored for morphological appearance at × 400 [after the method of Chalkley (16)]. Regions underlying a total of 200 randomly distributed points per tumor (10 points in 20 different fields) were graded as necrotic, cellular, interstitial, or vascular. All grading was done by a single individual (R. G. S.) having no knowledge of the sample identity.

RESULTS

Certain NMR-observable parameters are correlated with untreated tumor progression (Table 1). In untreated tumors the adenylate ratio decreased with time (β-NTP:γ-NTP ratio, $P < 0.001$), while the relative intensity of the phosphomonoester resonance increased (PME:α-NTP ratio, $P < 0.01$).

BCNU treatment arrested tumor volume growth for more than 4 days (data not shown). Representative *in vivo* spectra for BCNU-treated and sham-treated 9L gliosarcoma are shown 4 days after treatment (Fig. 1). At the time these spectra were taken, the untreated tumors were approximately 2.4 times larger in volume than the BCNU-treated tumors [volume at day 4; untreated = 8.4 ± (SD) 1.9 cm^3; treated = 3.5 ± 1.6 cm^3; $P < 0.005$).

A comparison of treated and sham-treated control tumors 1 day posttherapy showed that only the P_i:PCr ratio was significantly different ($P < 0.05$) (Table 2). However, 4 days posttreatment the treated tumors differed significantly from the controls in many respects. The most significant change following treatment was a decrease in the relative area of the PME resonance (PME:α-NTP, $P < 0.01$). The relative area of the P_i resonance also decreased in the treated tumors (P_i:α-NTP ratio, $P < 0.05$). The relative amount of PCr was more than twice as high in treated tumors (PCr:α-NTP, $P < 0.05$), while the relative amount of NTP increased (β-NTP:α-NTP ratio, $P < 0.05$) (Table 2). The tumor pH, calculated from the chemical shift of the P_i resonance (2), did not change during tumor progression or following tumor treatment. Although the volume of the treated tumor did not change significantly over the course of the NMR experiment, the relative amount of phosphocreatine in the treated tumor doubled between days 1 and 4 posttreatment (PCr:α-NTP ratio, day 1 = 0.16 to day 4 = 0.32, $P < 0.05$) (Table 2).

Analysis of treated and control tumors 4 days following treatment revealed no significant difference in the extent of macroscopic cyst formation. In treated tumor sections, the cystic regions occupied 21.0 ± 18.0% of the cross-sectional area, while in control tumor sections, cystic regions occupied 17.7 ± 2.3%. The difference in sample variances between treated and untreated tumors is significant (variance ratio test; $F = 61.2$; $P < 0.001$).

Histological sections of treated and control tumors 4 days following treatment were scored for size, abundance of blood vessel cross-sections, and density of tumor cells (Table 3). Untreated tumors had significantly more vessel cross-sections per field ($P < 0.001$), although these vessels were significantly smaller in diameter than in treated tumors ($P < 0.01$) (Figs. 2 and 3). There were more telangiectatic vessels or sinusoids in the treated tumor (vessels >40 μm; treated, 38.3%, control, 22.0%) (Fig. 4). The calculated vessel cross-sectional area per microscopic field was less in the treated tumors than in the control (Table 3). The number of cells per microscopic field was reduced by 30.8% following treatment with BCNU ($P < 0.001$) (Figs. 4 and 5). Because of this reduction in the number of cells per field in the treated tumors, the calculated value for number of cells per unit vessel area is roughly equal in the treated and control tumor sections.

Analysis of regions underlying 200 randomly chosen points per tumor showed significant differences between treated and control tumors in micromorphology (χ^2 test; $P < 0.001$) (Table 4). Cells were classified as necrotic when karyolysis was evident, with indefinite or absent cell margins or clear damage to the cytoplasmic membrane. Such cells often formed a confluent smear of cells with poorly stained or absent nuclei (Fig. 3). Calcification was occasionally visible in necrotic regions, and necrosis was clearly coagulative rather than liquefactive. Cells were classified as intact tumor cells when nuclear basophilia was evident in cells that were not endothelial cells. Intact cells lacked nuclear vacuolation and cell margins were well to poorly defined (Fig. 2). Extracellular space was defined as interstitial space, clear of acellular debris, necrotic cells, or cell fragments. Such space usually appeared as regions in which viable cells were surrounded by a mesh-like stroma (Figs. 4 and 5). Vessel lumens and vessel elements were separately scored but are excluded from this analysis because of their rarity. Glomeruloid endothelial hyperplasia was noted in 8 of 11 tumor sections (Fig. 5). Treated tumors had both a lower proportion of necrosis and 5 times as much extracellular space as the untreated control.

Table 1 ^{31}P *NMR spectroscopy of 9L tumors: untreated growth*

Spectra were obtained on various days after implantation. Resonance area ratios were calculated for each individual spectrum. Values presented are means ± SD for the indicated number of animals. For spectra in which the PCr resonance was below the limit of detection, a value of 1 was assigned, the largest resonance having been defined as 100. For this reason, ratios containing PCr may be indicated as limits.

Tumor age	PCr:α-NTP	P_i:α-NTP	PME:α-NTP	P_i:PCr	β-NTP:α-NTP	β-NTP:γ-NTP
7 days ($n = 5$)	0.19 ± 0.07	0.73 ± 0.63	0.54 ± 0.19	4.58 ± 4.89	0.62 ± 0.08	0.96 ± 0.19
13–14 days ($n = 13$)	<0.11 ± 0.10	1.19 ± 0.54	0.73 ± 0.19	>44.24 ± 46.37	0.43 ± 0.10	0.73 ± 0.15
17–18 days ($n = 5$)	<0.13 ± 0.12	1.82 ± 0.98	0.99 ± 0.20	>44.46 ± 50.84	>0.32 ± 0.22	0.47 ± 0.27
Correlation coefficient[a] ($n = 23$)						
$r =$	−0.196	0.487	0.619	0.377	−0.634	−0.665
$P <$	NS	0.01	0.01	NS	0.01	0.001

[a] Correlation coefficients were derived from the raw data by linear regression. The significance of the slope (P) was determined by t test. NS, not significant.

Table 2 *^{31}P NMR spectroscopy of 9L tumors: response to BCNU*

Comparison of resonance area ratios of spectra from age-matched treated and sham-treated (control) tumors. Animals were treated 12 days after tumor implantation and examined by NMR spectroscopy 1 and 4 days after treatment. Values are means ± SD of the resonance area ratios for the indicated number of animals.

	PCr:α-NTP	P_i:α-NTP	PME:α-NTP	P_i:PCr	β-NTP:α-NTP	β-NTP:γ-NTP
1 day posttreatment						
BCNU-treated 13–14 days (n = 12)	0.16 ± 0.13	0.92 ± 0.40	0.80 ± 0.34	11.29 ± 9.73	0.46 ± 0.10	0.73 ± 0.18
Control 13–14 days (n = 13)	<0.11 ± 0.10 NS[a]	1.19 ± 0.54 NS	0.73 ± 0.19 NS	>44.24 ± 46.37 [b]	0.43 ± 0.10 NS	0.73 ± 0.15 NS
4 days posttreatment						
BCNU-treated 17–18 days (n = 6)	0.32 ± 0.16	0.94 ± 0.33	0.71 ± 0.12	4.28 ± 3.66	0.53 ± 0.11	0.77 ± 0.14
Control 17–18 days (n = 5)	<0.13 ± 0.12 [b]	1.82 ± 0.98 [b]	0.99 ± 0.20 [c]	>44.46 ± 50.84 [b]	0.32 ± 0.22 [b]	0.47 ± 0.27 [b]

[a] NS, not significant.
[b] Significant ($P < 0.05$) difference between treated and age-matched controls by t test analysis.
[c] Significant ($P < 0.01$) difference between treated and age-matched controls by t test analysis.

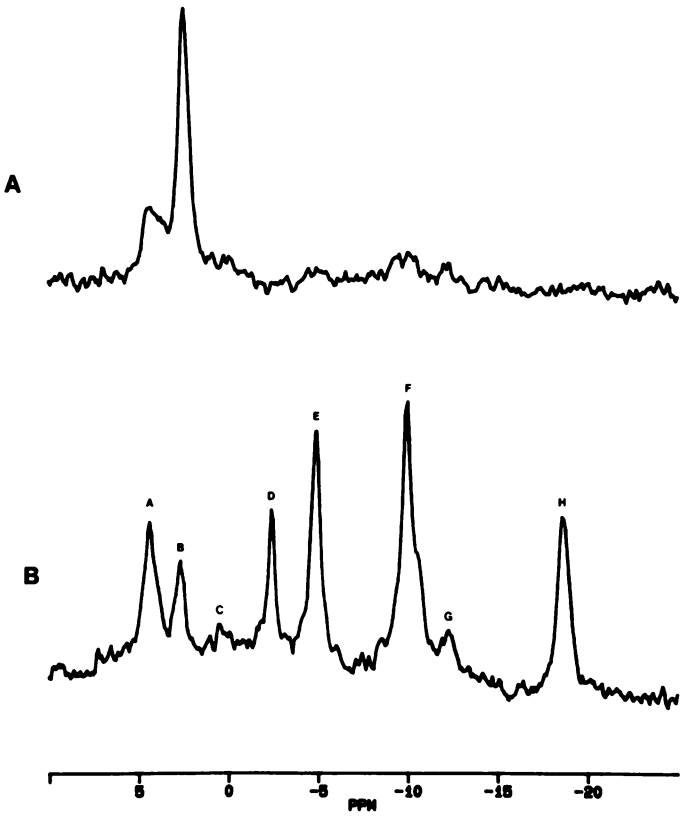

Fig. 1. *In vivo* spectra from s.c. implanted 9L gliosarcoma at day 16 postimplantation. (*A*) Spectrum from sham-treated control 4 days posttreatment. (*B*) Spectrum from BCNU-treated (10 mg/kg injected i.p.) rat tumor 4 days posttreatment. Identification of resonances by chemical shift, doping, and pH sensitivity are as follows: (*Peak A*) PEt and PCh; (*Peak B*) P_i; (*Peak C*) glycero-PEt and glycero-PCh; (*Peak D*) phosphocreatine; (*Peak E*) γ-NTP and nucleoside diphosphate β-phosphate; (*Peak F*) NTP and nucleoside diphosphate α-phosphates together with various other compounds such as NADPH/NADP and NADH/NAD; (*Peak G*) unknown, possibly UDPG; (*Peak H*) β-NTP.

DISCUSSION

We have identified several progressive changes in the ^{31}P NMR spectra of the untreated 9L gliosarcoma that are correlated with tumor growth. The most significant of these is the decline in the ratio of β-NTP to γ-NTP. In addition, the amount of P_i increases relative to α-NTP, while PCr:α-NTP tends to decrease, duplicating the pattern of metabolic decline described by Evanochko *et al.* (2). Lowry *et al.* (17) have shown that levels of PCr in human tumors vary directly with the tumor adenylate energy charge. Ng *et al.* (1) suggested that low levels of PCr and NTP are evidence for increasing proportions of hypoxic cells in a growing tumor. This hypothesis is consistent with our observation that large 9L tumors tend to have numerous microfoci of necrosis [see also Barker *et al.* (18)].

Tumor growth is correlated with a significant relative increase in the PME resonance. This resonance has been analyzed in perchloric acid extracts of 9L tumors. The *in vivo* resonance is contributed by PEt and PCh in roughly a 6:1 ratio (data not shown). Positive identification of the resonances was made by chemical shift in ^{31}P and ^{1}H spectra, by doping with authentic PEt and PCh in ^{31}P and ^{1}H spectra, and by analysis of a homonuclear two-dimensional ^{1}H correlated spectroscopy.[4] Phosphorylethanolamine is the major constituent of the PME peak in developing dog brain (19) and has also been identified in methanol extracts of human neuroblastoma biopsies (20). Maris *et al.* (20) note that increases in the relative amount of PME are associated with rapid progression of neuroblastoma in children and that successful tumor treatment is associated with a decline in the intensity of the PME resonance. Friend erythroleukemia cells inoculated s.c. in mice induce tumors with elevated NMR resonances of PEt and PCh which decreased in response to i.t. administration of interferon (21). Regression of these resonances served as an early marker of interferon-induced tumor regression, inasmuch as NMR changes preceded formation of necrotic areas in the tumor (21). Changes in the PME resonance may be associated with membrane turnover in rapidly proliferating tissue (20–22).

Following chemotherapy with BCNU, NMR spectra of 9L gliosarcoma indicate that a significant metabolic reenergization occurs. It is unlikely that the increase in PCr reported here is a result of increased signal contribution from the body wall because the volume of the tumor did not decrease significantly during the observation period. Therefore the observed reenergization is occurring in the tumor itself. This reenergization of the tumor could result from one or several different effects: (*a*) chemotherapy may directly affect tumor vasculature resulting in increased blood flow to the tumor; (*b*) cell killing may decrease i.t. hydrostatic pressure and improve blood flow; (*c*) cell killing may reduce competition for oxygen; (*d*) preferential killing of low energy cells or recruitment of quiescent cells into a metabolically more active form may enhance the fraction of energized cells contributing to the spectrum; (*e*) killing of some fraction of the tumor may induce an inflammatory response, recruiting macrophages into the tumor and resulting in invasion of the tumor by normal cells.

We have tested some of these hypotheses by a quantitative histological analysis of microscope slide mounts of treated and untreated 9L tumors. To test the hypothesis that changes in the treated tumor spectra were associated with changes in the

[4] R. G. Steen, K. A. McGovern, R. J. Tamargo, and J. D. Glickson, manuscript in preparation.

Table 3 *Vascularization of 9L tumors: response to BCNU*

Histological comparison of BCNU-treated and age-matched, sham-treated control 9L tumors. Individual tumor sections were scored for vessel cross-sections per field, with vessels in cross-section or longitudinal section counted if endothelial cells lining the vessel lumen were visible and RBC were present in the lumen. Vessel maximum diameter was measured with an ocular micrometer, and vessel cross-sectional area per field was calculated by assuming each vessel to be cylindrical. Cells per field were estimated by counting intact nuclei per field. The number of cells per unit vessel cross-sectional area was calculated from the two measured values. Values are mean ± SD.

	Vessel cross-sections/field[a]	Vessel diameter[b] (μm)	Vessel cross-sectional area/field (μm × 10^{-3})	Cells/field[c] (× 10^{-3})	Cells/vessel area (cells/μm^2)
BCNU-treated (6 tumors)	3.60 ± 3.10	44.93 ± 40.58	5.70	33.03 ± 5.00	5.79
Controls (5 tumors)	8.16 ± 8.49[d]	33.68 ± 26.63[e]	7.27	47.75 ± 11.74[d]	6.57

[a] Forty samples per tumor were examined.
[b] Twenty samples per tumor were examined.
[c] Five samples per tumor were examined.
[d] Significant ($P < 0.001$) difference between treated and age-matched controls by *t* test analysis.
[e] Significant ($P < 0.01$) difference between treated and age-matched controls by *t* test analysis.

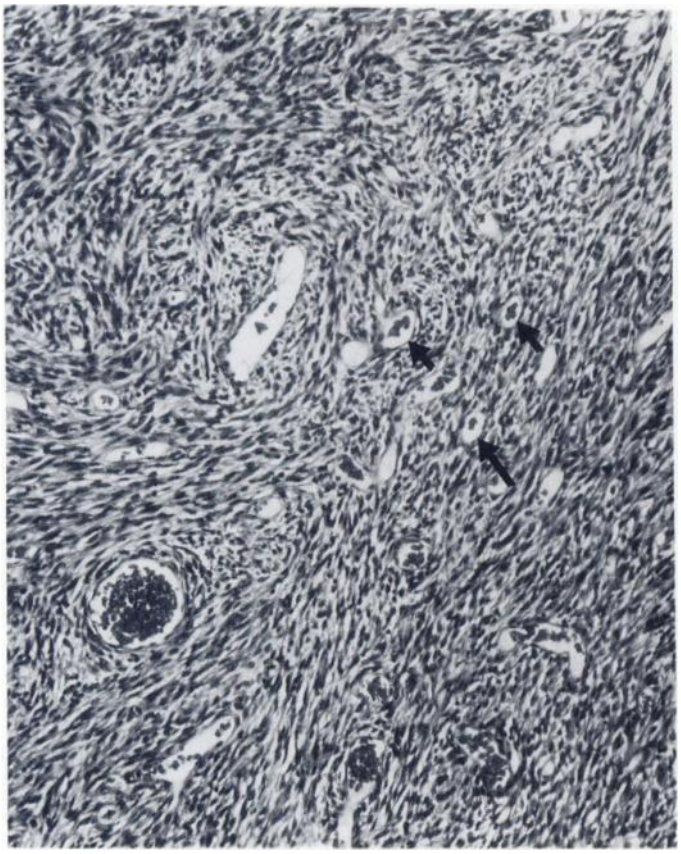

Fig. 2. Histological section of control 9L tumor 4 days after sham treatment. Note the dense field of cells with hyperchromatic nuclei and the numerous capillaries cut in cross- or oblique section (*arrows*).

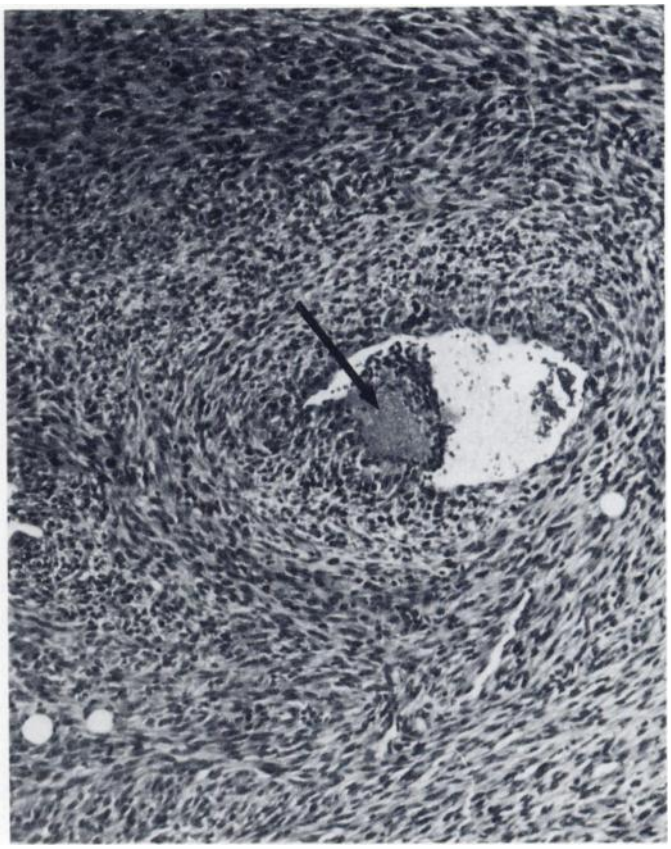

Fig. 3. Histological section of control 9L tumor 4 days after sham treatment. Note the large central area of coagulative necrosis, with necrotic cells forming a confluent smear of enucleated cells (*arrow*). Adjacent to this necrotic region is a small cystic pocket.

tumor vasculature, we calculated the average number of cells per unit vessel cross-sectional area. The results (Table 3) do not reveal a quantitative difference in vascular area per cell between treated and untreated tumor sections. We note that this analysis is not sensitive to treatment-induced changes in permeability of the vessel walls, changes in flow rates in the vessels *in vivo*, or changes in extravascular perfusion.

To test the hypothesis that spectral changes in treated tumors were associated with killing of some subpopulation of cells, we analyzed the tumor sections for changes in tumor micromorphology. Histological analysis is insufficient to determine whether a proliferating fraction was killed and a quiescent fraction then recruited into the cell cycle, or whether cells already partially hypoxic were killed and cleared, leaving the proliferating cells. However, this analysis clearly demonstrates profound changes following treatment. Treated tumor sections were characterized by having fewer microfoci of necrosis, more viable cells, and a 5-fold increase in interstitial space (Table 4). The changes in interstitial space reported here after treatment of 9L with BCNU are similar to changes described in other tumor models. Three days following treatment of a murine sarcoma with X-irradiation, tumor interstitial volume increased 29% while the tumor cells underwent a compensatory decrease in volume (23). Intervals of increased tumor cell proliferation following subcurative therapeutic insult may be accompanied by profound changes in interstitial water volumes in the RIF-1 murine fibrosarcoma (24).

We examined tumor histological sections for evidence of macrophage infiltration, to test whether tumor reenergization

Fig. 4. Histological section of BCNU-treated (10 mg/kg) 9L tumor 4 days after treatment. Note the dense field of cells grading into a region depleted of cells but with abundant interstitial space. Several telangiectatic vessels (*arrows*) are visible in cross-section at the *lower right*.

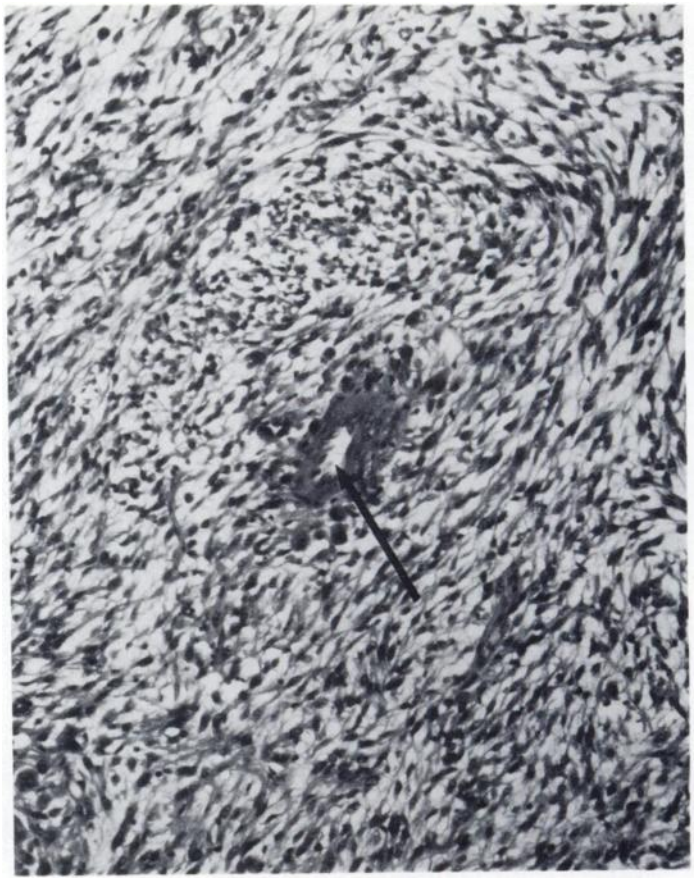

Fig. 5. Histological section of BCNU-treated (10 mg/kg) 9L tumor 4 days after treatment. Note the hypertrophied endothelial cells in the capillary (*arrow*) and the abundant interstitial space in the surrounding field of cells. Individual observations (200/section) were cross-classified and analyzed by a χ^2 test of independence. This analysis indicates that drug treatment has a significant effect on tumor histology ($P < 0.001$).

Table 4 *Micromorphology of 9L tumor: response to BCNU*

Histological comparison of BCNU-treated and sham-treated control 9L tumors 4 days posttreatment. Dots were randomly placed on the microscope ocular so that points were projected onto the field of cells; randomly selected fields were then scored by classifying the regions of the tumor lying directly under the points. Individual observations (200/section) were cross-classified and analyzed by a χ^2 test of independence.

	Observations		
	Necrotic cells	Intact cells	Extracellular space
BCNU-treated[a]	541 (45.9)[b]	452 (38.3)	187 (15.9)
Controls[c]	634 (65.7)	299 (31.0)	32 (3.3)
	$\chi^2 = 128.0$; $P < 0.001$		

[a] A total of 1180 points from 6 treated tumors were scored.
[b] Numbers in parentheses, percentage.
[c] A total of 965 points from 5 treated tumors were scored.

was due to an inflammatory response and the recruitment of normal cells into the tumor. No evidence of macrophage or polymorphonuclear infiltration was seen, nor was perivascular cuffing seen in any of the sections examined. This finding is consistent with earlier histological observations of the BCNU-treated 9L tumor (25). However, examination of histological sections of treated and untreated tumors suggested that there may have been qualitative changes in the morphology of intact appearing cells. Untreated tumors showed a fascicular growth pattern, with swirling bands of spindle-shaped cells. In the treated tumor sections there seemed to be a shift from a sarcomatous to a more gliomatous morphology. The significance of such a change is unknown.

Metabolite concentrations and pH values determined by NMR spectroscopy of tumors are not uniform characteristics of identical cells but represent average values for an often heterogeneous population (3). The changes in the proportions of viable and necrotic cells reported here could be sufficient to account for the differences in NMR spectra following treatment, although changes in blood flow and oxygenation may also be involved. Our results show that BCNU given in moderate doses [75% of a 10% lethal dosage for adult Fischer 344 rats (26)] produces a metabolic reenergization of the tumor. Although at this dose the observed metabolic reenergization could reflect the eventual recurrence of the tumor, a similar effect was reported in preliminary work with the MOPC 104E myeloma given a curative dose of BCNU (1).

ACKNOWLEDGMENTS

The authors wish to thank C. Paella Martin for careful reading of the manuscript and S-J Li and W. O'Loughlin for helpful discussions.

REFERENCES

1. Ng, T. C., Evanochko, W. T., Hiramoto, R. N., Ghanta, V. K., Lilly, M. B., Lawson, A. J., Corbett, T. H., Durant, J. R., and Glickson, J. D. ^{31}P NMR spectroscopy of *in vivo* tumors. J. Magn. Reson., *49:* 271–286, 1982.
2. Evanochko, W. T., Ng, T. C., Lilly, M. B., Lawson, A. J., Corbett, T. H., Durant, J. R., and Glickson, J. D. *In vivo* ^{31}P NMR study of the metabolism of murine mammary 16/C adenocarcinoma and its response to chemotherapy, X-radiation, and hyperthermia. Proc. Natl. Acad. Sci. USA, *80:* 334–338, 1983.
3. Wehrle, J. P., Li, S.-J., Rajan, S. S., Steen, R. G., and Glickson, J. D. ^{31}P and ^{1}H NMR spectroscopy of tumors *in vivo*: untreated growth and response to chemotherapy. Ann. NY Acad. Sci., in press, 1988.
4. Evanochko, W. T., Ng, T. C., and Glickson, J. D. Application of *in vivo* NMR spectroscopy to cancer. Magn. Reson. Med., *1:* 508–534, 1984.

5. Glickson, J. D., Evanochko, W. T., Sakai, T. T., and Ng, T. C. *In vivo* NMR spectroscopy of tumors. *In:* R. K. Gupta (ed.), NMR Spectroscopy of Cells and Organisms. Boca Raton, FL: CRC Press, 1987.
6. Gadian, D. G. Nuclear Magnetic Resonance and Its Application to Living Systems. Oxford, United Kingdom: Oxford University Press, 1982.
7. Evanochko, W. T., Sakai, T. T., Ng, T. C., Krishna, N. R., Kim, H. D., Zeidler, R. B., Ghanta, V. K., Brockman, R. W., Schiffer, L. M., Braunschweiger, P. B., and Glickson, J. D. NMR study of *in vivo* RIF-1 tumors: analysis of perchloric acid extracts and identification of ^{1}H, ^{31}P and ^{13}C resonances. Biochim. Biophys. Acta, *805:* 104–116, 1984.
8. Navon, G., Ogawa, S., Shulman, R. G., and Yamane, T. ^{31}P NMR studies of Ehrlich ascites tumor cells. Proc. Natl. Acad. Sci. USA, *74:* 87–91, 1977.
9. Naruse, S., Hirakawa, K., Horikawa, Y., Tanaka, C., Higuchi, T., Ueda, S., Nishikawa, H., and Watari, H. Measurements of *in vivo* ^{31}P nuclear magnetic resonance spectra in neuroectodermal tumors for the evaluation of the effects of chemotherapy. Cancer Res., *45:* 2429–2433, 1985.
10. Evanochko, W. T., Ng, T. C., Glickson, J. D., Durant, J. R., and Corbett, T. H. Human tumors as examined by *in vivo* ^{31}P NMR in athymic mice. Biochem. Biophys. Res. Commun., *109:* 1346–1352, 1982.
11. Schiffer, L. M., Braunschweiger, P. B., Glickson, J. D., Evanochko, W. T., and Ng, T. C. Preliminary observations on the correlation of proliferative phenomena with *in vivo* ^{31}P NMR spectroscopy after tumor chemotherapy. Ann. NY Acad. Sci., *459:* 270–277, 1985.
12. Ovejera, A., Houchens, D. P., and Barker, A. D. Chemotherapy of human tumor xenografts in genetically athymic mice. Ann. Clin. Lab. Sci., *8:* 50–56, 1978.
13. Bullard, D. E., Schold, S. C., Bigner, S. H., and Bigner, D. D. Growth and chemotherapeutic response in athymic mice of tumors arising from human glioma-derived cell lines. J. Neuropathol. Exp. Neurol., *40:* 410–427, 1981.
14. Ng, T. C., and Glickson, J. D. Shielded solenoidal probe for *in vivo* NMR studies of solid tumors. Magn. Reson. Med., *2:* 169–175, 1985.
15. Rajan, S. S., Wehrle, J. P., and Glickson, J. D. A novel double tuned circuit for *in vivo* NMR. J. Magn. Reson., *74:* 147–154, 1987.
16. Chalkley, H. W. Method for the quantitative morphologic analysis of tissues. J. Natl. Cancer Inst., *4:* 47–53, 1943.
17. Lowry, O. H., Berger, S. J., Chi, M. M.-Y., Carter, J. G., Blackshaw, A., and Outlaw, W. Diversity of metabolic patterns in human brain tumors—I. High energy phosphate compounds and basic composition. J. Neurochem., *29:* 959–977, 1977.
18. Barker, M., Hoshino, T., Gurcay, O., Wilson, C. B., Nielsen, S. L., Downie, R., and Eliason, J. Development of an animal brain tumor model and its response to therapy with 1,3-bis(2-chloroethyl)-1-nitrosourea. Cancer Res., *33:* 976–986, 1973.
19. Gyulai, L., Bolinger, L., Leigh, J. S., Barlow, C., and Chance, B. Phosphorylethanolamine—the major constituent of the phosphomonoester peak observed by ^{31}P-NMR on developing dog brain. FEBS Lett., *178:* 137–142, 1984.
20. Maris, J. M., Evans, A. E., McLaughlin, A. C., D'Angio, G. J., Bolinger, L., Manos, H., and Chance, B. ^{31}P nuclear magnetic resonance spectroscopic investigation of human neuroblastoma *in situ*. N. Engl. J. Med., *312:* 1500–1505, 1985.
21. Proietti, E., Carpinelli, G., DiVito, M., Belardelli, F., Gresser, I., and Podo, F. ^{31}P-nuclear magnetic resonance analysis of interferon-induced alterations of phospholipid metabolites in interferon-sensitive and interferon-resistant Friend leukemia cell tumors in mice. Cancer Res., *46:* 2849–2857, 1986.
22. Agris, P. F., and Campbell, I. D. Proton nuclear magnetic resonance of intact Friend leukemia cells: phosphorylcholine increase during differentiation. Science (Wash. DC), *216:* 1325–1327, 1982.
23. Peterson, H. I., Appelgren, L., Kjartansson, I., and Selander, D. Vascular and extravascular spaces in a transplantable rat tumor after local X-ray irradiation. Z. Krebsforsch., *87:* 17–25, 1976.
24. Braunschweiger, P. G., Schiffer, L., and Furmanski, P. The measurement of extracellular water volumes in tissues by gadolinium modification of ^{1}H-NMR spin lattice (T1) relaxation. Magn. Reson. Imaging, *4:* 285–291, 1986.
25. Rosenblum, M. L., Knebel, K. D., Vasquez, D. A., and Wilson, C. B. *In vivo* clonogenic tumor cell kinetics following 1,3-bis(2-chloroethyl)-1-nitrosourea brain tumor therapy. Cancer Res., *36:* 3718–3725, 1976.
26. Bullard, D. E., Bigner, S. H., and Bigner, D. D. Comparison of intravenous *versus* intracarotid therapy with 1,3-bis(2-chloroethyl)-1-nitrosourea in a rat brain tumor model. Cancer Res., *45:* 5240–5245, 1985.